Final Report on

Analysis of Triangular Arrays of Josephson Tunnel Junctions*

P. Caputo and A. V. Ustinov

Physikalisches Institut III, Universität Erlangen-Nürnberg
D-91054 Erlangen, Germany

* Supported by Air Force Office of Scientific Research (AFOSR)
under Contract F61775-98-WE041.

May 1999

REPORT DOCUMENTATION PAGE

Form Approved OMB No. 0704-0188

1. AGENCY USE ONLY (Leave blank)	2. REPORT DATE	3. REPORT TYPE AND DATES COVERED
	May 1999	Final Report

4. TITLE AND SUBTITLE

Analysis of Triangular Arrays of Josephson Tunnel Junction

5. FUNDING NUMBERS

F61775-98-WE041

6. AUTHOR(S)

Prof. Alexey Ustinov

7. PERFORMING ORGANIZATION NAME(S) AND ADDRESS(ES)

Department of Physics University of Erlangen-Nuremberg
University of Erlangen-Nuremberg
Erwin-Rommel-Str. 1
Erlangen 91058
Germany

8. PERFORMING ORGANIZATION REPORT NUMBER

N/A

9. SPONSORING/MONITORING AGENCY NAME(S) AND ADDRESS(ES)

EOARD
PSC 802 BOX 14
FPO 09499-0200

10. SPONSORING/MONITORING AGENCY REPORT NUMBER

SPC 98-4022

11. SUPPLEMENTARY NOTES

12a. DISTRIBUTION/AVAILABILITY STATEMENT

Approved for public release; distribution is unlimited.

12b. DISTRIBUTION CODE

A

13. ABSTRACT (Maximum 200 words)

This report results from a contract tasking Department of Physics University of Erlangen-Nuremberg as follows: The contractor shall perform an experimental study of triangular arrays of Josephson tunnel junctions operating in a magnetic field. The experimental samples will be designed on the bases of theoretical ideas suggested by Yukon and Lin to use multi-row (two-dimensional) triangular arrays as microwave sources. In addition, the contractor shall perform the following tasks: 1) test the scaling of power in single-row arrays with the number of emitting junctions and to make measurements of the linewidth of the emitted radiation, 2) make comparative study of triangular arrays with different damping in the junctions and with different geometry of the cell, in order to enhance the emitted power, 3) make systematic RF characterization of double-row arrays.

14. SUBJECT TERMS	15. NUMBER OF PAGES
EOARD, Optical Components, Optical Diagnostics	14
	16. PRICE CODE N/A

17. SECURITY CLASSIFICATION OF REPORT	18. SECURITY CLASSIFICATION OF THIS PAGE	19. SECURITY CLASSIFICATION OF ABSTRACT	20. LIMITATION OF ABSTRACT
UNCLASSIFIED	UNCLASSIFIED	UNCLASSIFIED	UL

Contents

Abstract

High frequency properties of underdamped Josephson junction arrays consisting of two rows of parallel biased cells are studied experimentally. Two row arrays of different geometries are investigated and compared with respect of their microwave power in the W-band. Comparative measurements have shown that, among the studied configurations, the best performance is obtained from an array with square cells and two horizontal junctions. In this array, the measured output power is up to 2 times larger than that in the array with only one horizontal junction, and up to 20 times larger with respect to the array with conventional triangular cells. Experimental data are in good qualitative agreement with previously reported numerical simulations of Yukon and Lin. We confirm that in square cell arrays an enhanced rf voltage can be extracted from the horizontal junctions.

Introduction

Triangular arrays of Josephson tunnel junctions have been shown to be suitable for high frequency applications in the mm and sub-mm range [1]. Their application is based on the property that, at the applied field corresponding to half a flux quantum in every cell ($f = 0.5$), the junctions transverse to the forcing current (*horizontal* junctions) perform small amplitude oscillations about their equilibrium state, yielding an rf power with very small content of higher harmonics while the dc voltage remains equal to zero. The *vertical* junctions rotate under the driving force from the external bias current, developing a dc voltage different from zero. The oscillations of the horizontal junctions are at a frequency equal to the Josephson frequency of the vertical junctions. The radiation emitted by the horizontal junctions has been measured in a frequency range of 90 - 100 GHz and the typical delivered power was about 90 pW. A linewidth as small as 80 MHz at about 86 GHz has been measured [2].

Radiation from the horizontal junctions of a *two*-row array has been already seen earlier[2]. In this geometry, the junctions coupled to the antenna are the ones placed in the middle line of the array. At frustration $f = 0.5$, a voltage locking of the rows was found, but a small deviation from $f = 0.5$ destroyed the locked state. The radiation power was found to be smaller than that measured in single row arrays. The FFT analysis of the simulated array has shown that the rf voltage consists of many frequency components. This behavior differs both from the pure checkerboard state, at which the array is supposed to deliver maximum of power from the horizontal junctions, and from the pure ribbon state, at which the horizontal junctions do not oscillate at all. This novel state was called "mixed" state, since several components at fairly close frequencies are found there.

Recently, we have studied two row arrays which were designed on the basis of results established in numerical investigations. These simulations performed by N. C. Lin and S. Yukon[3] have shown that a more reliable and stable checkerboard state might be achieved if the *conventional* two row array (*cf.* the geometry studied in the previous report[4]) is slightly modified. First of all, it was shown that having an odd number of triangular cells per row might enhance the rf voltage with respect to the case of even number of

cells per row. Moreover, the numerics has established that adding some extra cells, here called *tabs*, to the top and bottom sides of all the odd columns enlarges the region in the I-V curve where the checkerboard state is found. The reason of this might be that this arrangement reduces the circulating currents that destroy the phase locking between the rows. Another point which has been shown to be essential for getting a pure checkerboard state is replacing every horizontal junction by two junctions in series. This extra junction is expected to double the horizontal rf voltage that we extract from the array.

We have prepared a new layout where the above ideas are explored. In the two row array chips, the following devices have been included:

- arrays with odd number of cells and tabs
- arrays constructed with one horizontal junction (square and triangular cells) and with two horizontal junctions (square cells)
- arrays with two horizontal junctions and different number of cells (7 and 13).

Here we present an outcome of experiments. The optimal operation of a triangular array is when the damping in the junctions is relatively high (McCumber parameter $\beta_c \approx 3 - 5$). Our junctions are underdamped, though we increase the damping by operating at higher temperatures. Unfortunately, in this regime, the temperature fluctuations often degrade the rf output. The use of junctions shunted on-chip by resistors allows to have the desired damping range, avoiding higher temperatures. The drawback of on-chip shunting is the increased cell area and, therefore, too large discreteness parameter β_L. Radiation measurements of shunted arrays are presently in progress.

Samples and dc measurements

We have characterized several types of two row arrays of Josephson junctions. Figure 1 shows a sketch of the investigated structures. The junctions consist of a Nb/Al-AlO_x/Nb trilayer and have a critical current density of about 1000 A/cm^2[5]. Their area is designed to be 9 μm^2. The arrays consist of two rows of cells, where the junctions are arranged in either triangular lattice (with 3 junctions per elementary cell) or square lattice (with 4 junctions per elementary cell). In the triangular lattice, the elementary cell is either a triangle [Fig. 1(a)] or a square [Fig. 1(b)]. The peculiarity of the square lattice is that the 4 junctions are not symmetrically placed along the perimeter of the square cell, but the top horizontal junction has been slid down beside the bottom horizontal junction (or vice versa). This junction arrangement is sketched in Fig. 1(c). All arrays have an odd number of cells per row (7 or 13) and the same cell size A (about 170 μm^2). The current I_b is injected through bias resistors of 35 Ω, to have an uniform bias distribution along the whole array. In addition, some extra insulated cells (tabs) are placed to the top and bottom sides of all the odd columns.

Important parameters are the array discreteness and the junction damping. The discreteness parameter is $\beta_L = 2\pi L I_c/\Phi_0$, where L is the self-inductance of the elementary cell, I_c is the junction critical current and Φ_0 is the magnetic flux quantum. The cell inductance is estimated as $L = 1.25\,\mu_0\sqrt{A}$, where μ_0 is the magnetic permeability. At $T = 4.2$ K, typical values of β_L are about 3. At the working temperature of about 6.5 K (estimated from the gap voltage), $\beta_L \approx 0.7$. The damping is defined by the McCumber parameter, $\beta_c = 2\pi I_c R_N{}^2 C/\Phi_0$. Here R_N is the subgap resistance and C is the junction capacitance. At $T = 4.2$ K, typical values of β_c are around 1000 and larger (underdamped limit). At the working temperature of about 6.5 K, $\beta_c \approx 1$.

The series-connected horizontal junctions placed in the central line of the arrays are coupled to a finline antenna, used to match the impedance of the junctions to the impedance of the external rectangular waveguide. The finline antenna is made of two exponentially tapered Nb fins that are vertically separated by 0.5 μm thick SiO_2 layer. For a given dielectric constant ϵ_r, the impedance of a stripline is a function of w/h, the ratio

of the stripline width w to the dielectric height h (we have evaluated the impedance by using Wheeler's formula [6]). Due to fabrication rules, the thickness h of the insulating layer cannot be changed. Thus, only the overlapping area of the two superconducting fins allows to change the impedance of the transmission line. A simple evaluation of the junction impedance has been done considering each junction as a parallel connection of two elements with resistance R_N and the capacitance C. Thus, in order to provide good impedance matching between the stripline and the series-connected junctions, we have changed the overlap of the antenna electrodes proportionally to the number of the horizontal junctions present in the row.

The array behavior is studied in the presence of an external magnetic field, applied perpendicularly to the cell plane. The field is expressed in terms of the frustration f, defined as the magnetic flux threading the cell normalized to Φ_0. The experimental set-up used for dc and rf measurements and for data acquisition has been described in detail in the iterim report [4].

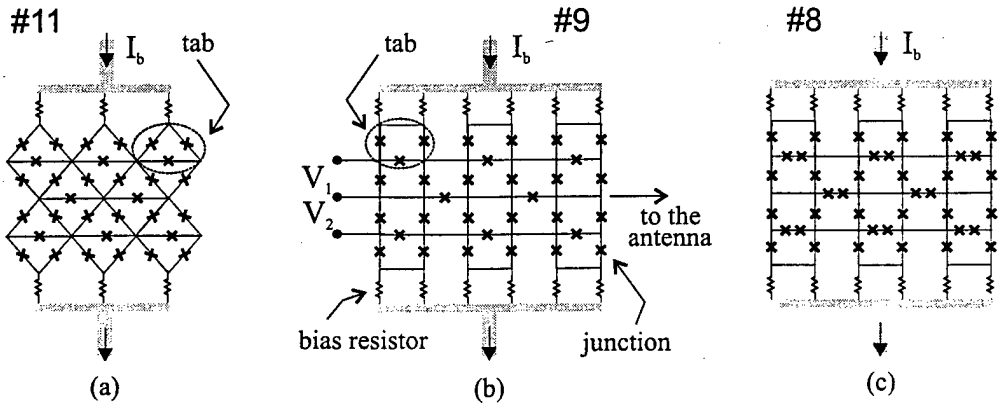

Figure 1: Schematic of the two row arrays with 5 cells per row: (a) triangular array with 3 junctions per cell (sample #11); (b) square array with 3 junctions per cell (sample #9); (c) square array with 4 junctions per cell (sample #8). The arrays are biased through resistors and tabs. The dc voltages V_1 and V_2 are measured across individual rows. The series-connected horizontal junctions in the central line are coupled to a finline antenna for detection of the rf voltage.

Before starting high frequency measurements, we have have characterized the dc properties of the new geometries. The sample consists of two rows of seven square cells, each cell containing four small Josephson junctions [see the schematic in Fig. 1(c)]. Typical I-V characteristics at $T = 4.2$ K is shown in Fig. 2(a). Current is injected through the bias resistors and tabs, and the individual row dc voltages are measured. Each single row exhibits very similar I-V characteristics. In the presence of frustration, the two typical

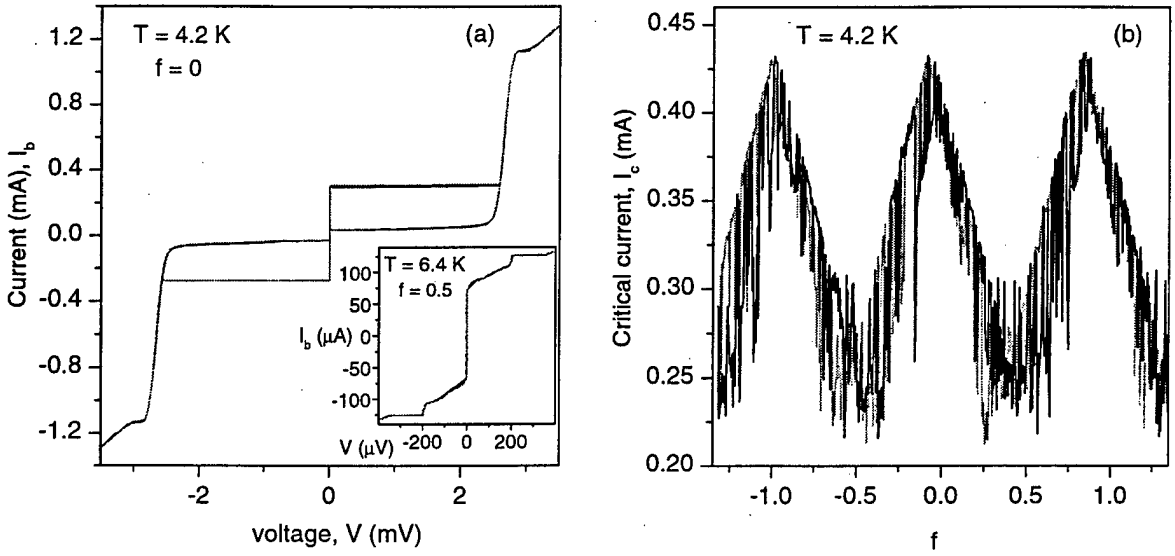

Figure 2: (a) Current-voltage characteristics of the two individual rows of the array sketched in Fig. 1(b) (#2993D-2). The two curves (gray and black lines) are very similar and overlap almost completely. Inset shows the enlargement of the low voltage region at $T = 6.4$ K ($\beta_c \approx 1.2$). Both rows are at the LC-resonance, which has the maximum voltage of about $200\,\mu$V at $f = 0.5$. (b) Dependencies of the row critical currents (gray and black lines) vs frustration.

steps appear in the I-V curves of the array. The asymptotic voltage position of the steps is field dependent and approaches the maximum value at $f = 0.5$. In the underdamped regime ($T = 4.2\,\mathrm{K}$), these resonances are not present in the I-V curve, and become stable only when $\beta_c \approx 2 - 3$ and smaller. The inset of Fig. 2(a) shows the upper resonance at $f = 0.5$. Here the two rows are found to be voltage locked. The rf horizontal voltage has been measured when the array is in this dynamical state (see next section). The $I_c(f)$ dependence of the array is similar to the previously studied geometries. The row critical currents are nearly equal and are modulated simultaneously by the applied magnetic field. Figure 2(b) shows typical patterns. Strong oscillations might be an indication of the existence of various metastable superconducting states from which the switch to the gap state takes place. These metastable states might be due to both the presence of more than three junction per cell and the relatively large self-inductance. We have experienced that increasing the temperature causes the reduction of these oscillations in the $I_c(f)$ curve, and when the temperature is such that $\beta_c \approx 2 - 3$ none of these oscillations is present in the pattern.

Radiation measurements

We have characterized the rf properties of two row arrays at the LC-resonance and at frustration $f \approx 0.5$. The frequency ν_J of the emitted radiation is expected to be given by the Josephson relation $\nu_J = V/\Phi_0$, where V is the dc voltage developed across one row. In order to evaluate the power level, the emitted radiation at the frequency ν_J is mixed to the signal of the Back Wave Oscillator (BWO) at a reference frequency $\nu_{\rm ref}$, and the output signal at the intermediate frequency $\nu_{IF} = \nu_J - \nu_{\rm ref}$ is amplified and sent to a calibrated power meter. The power meter is a diode power sensor which allows to measure power levels in a range 100 pW to 10 μW, in a frequency interval from 50 MHz to 26 GHz. The band of our IF amplifier was 0.4-1.3 GHz. The power meter has an analog output signal proportional to the measured power level, that we acquired by a computer. The typical recorded rf power vs. current is shown in Fig. 3.

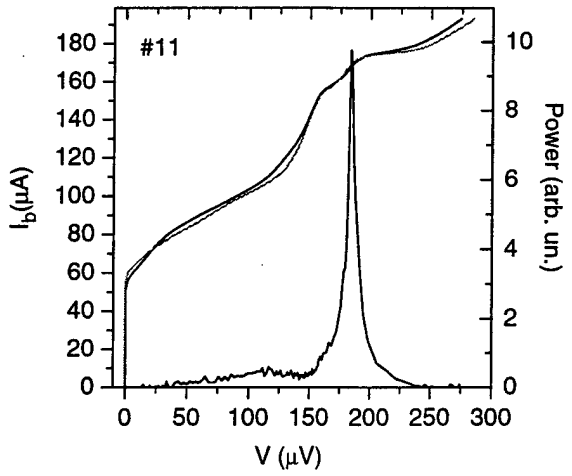

Figure 3: Current-voltage characteristics of the two individual rows of the array #2993D-11 (gray and black lines) and detected power at the reference frequency $\nu_{\rm ref} = 88$ GHz. The peak corresponds to an IF power of 20 nW (after IF amplification).

We have performed comparative rf measurements of the two row arrays sketched in Fig. 1, in order to find the optimal geometry which maximizes the microwave emission.

The dynamical state that we are interested in has the asymptotic voltage of about $200\,\mu$V, which corresponds to a Josephson frequency $\nu_J \approx 100\,$GHz. Therefore, the arrays have been characterized in the range frequency $\nu_{\rm ref} = 82 - 104\,$GHz. The experimental technique was the following:

1. First we check the individual row $I_c(f)$ dependencies to make sure that there is no residual magnetic flux trapped in the array.
2. Measure the individual row I-V curves to find both rows in a voltage-locked state
3. Find the optimum temperature to stabilize the resonance at $f = 0.5$
4. Record the emitted power vs. current at several (about 10-12) values of the reference frequency $\nu_{\rm ref}$.

Due to thermal fluctuations, the power peak could have changes of few percent from run to run. Thus, for a given $\nu_{\rm ref}$, we recorded several (5-7) sweeps of the I-V curve and made the average of the power level values. The mean-square error is reported in the plots.

As discussed above, in the design the finline antenna impedance has been scaled proportionally to the number of the series-connected junctions, i.e. according to the number of cells in the row (7 and 13) and to the cell type (with 1 or 2 horizontal junctions). Thus, for each of the studied geometries, we report the value of the estimated junction impedance, Z_d, and the width of the overlap of the finline electrodes, w.

In the following graphs we have summarized the data relative to the emitted power of the studied two row arrays (see Fig. 1). All the studied samples have 13 cells per row, except the sample #10 which has 7 cells. The sample #11 (with 3 JJ triangular cells) presents the LC resonance at slightly lower voltages. In the sample #9 (with 3 JJ square cells) the I-V curves of the individual rows have different subgap resistances, and it has been not always possible to lock the rows at the same voltage. Except for the latter case, in all the other arrays the row parameter spread has been small and also from sample to sample arrays were rather similar. That, in our opinion, justifies a comparison of the emitted power.

Figure 4(a) shows the detected power in the array #11 (with 3 JJ triangular cells, and in total 6 series-connected horizontal junctions). The asymptotic voltage of the step is found to be at slightly lower voltages; the maximum IF power is detected at $\nu_{\rm ref} = 87\,$GHz where it is about 21 nW. The array #9 (3 JJ square cells) is essentially the same as #11, the only difference being the geometry of the elementary cell (a square and not a triangle). In this case the maximum IF power of about 140 nW was detected, and this power level

was maintained in a large frequency range [see Fig. 4(b)]. An rf voltage about twice as large was measured in the array #8, where one more horizontal junction is added respect to the array #9. Now 12 are the horizontal junctions. A power up to 340 nW was measured, at $\nu_{\rm ref} = 92\,{\rm GHz}$ [see Fig. 4(c)]. We note, however, that for this sample the impedance of the finline antenna was scaled in order to match the different impedance of the series of junctions. In Fig. 4(d) the data for the array #10 are plotted. This sample is the same as #8 [Fig. 4(c)], but with less cells per row (7 vs. 13, i.e. 6 horizontal junctions vs. 12). In this case the maximum power of only about 50 nW was detected at $\nu_{\rm ref} = 92\,{\rm GHz}$.

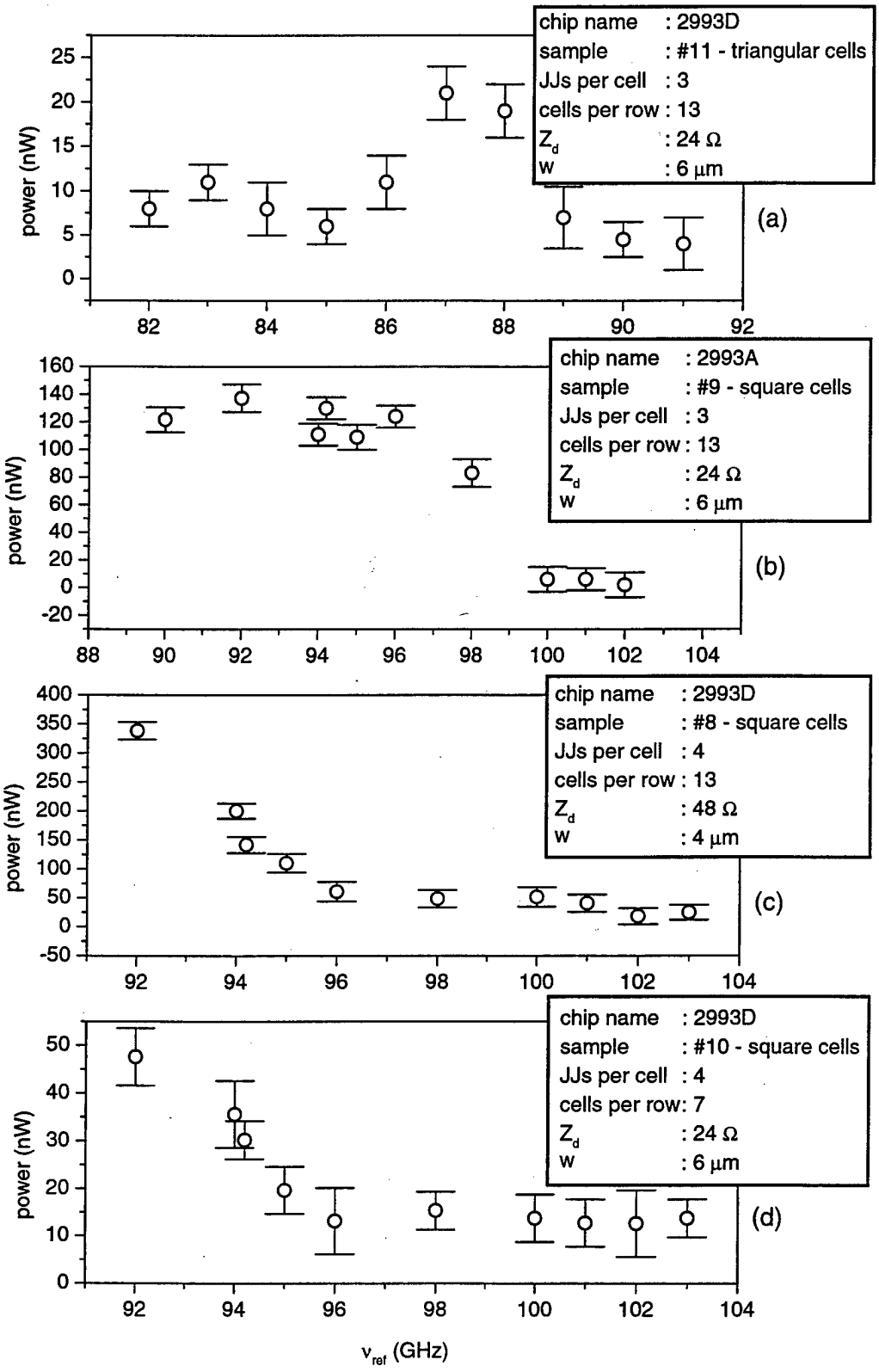

Figure 4: rf power at various reference frequencies in the different two row arrays. The power scale is referenced to the *amplified* IF level.

Conclusion

We have performed measurements of radiation emitted by the horizontal junctions of two row arrays. In order to enhance the rf power, new geometries have been studied. In summary, our data show that **(i)** arrays with square cells can deliver rf power higher than arrays with triangular cells; **(ii)** in the square version with 2 horizontal junctions the ac power is enhanced by a factor of about 2 with respect to the square cell with 1 horizontal junction; **(iii)** a power difference by a factor as large as 7 is found between the long square array (13 cells, 12 horizontal junctions), and the short square array (7 cells, 6 horizontal junctions). These results are, in general, in good agreement with what has been predicted in numerical simulations. The geometry shown in Fig. 1(c) has been already proposed and seems to be most promising for applications of triangular arrays as oscillators in active antenna[7].

For final definite conclusion, we would like to confirm the above experimental results with more samples, and, eventually, in a better thermally stabilized environment. Measurements of the scaling of power as a function of the number of the series-connected junctions in more simple systems, such as the single row arrays, are in progress, as well as radiation measurements of shunted arrays.